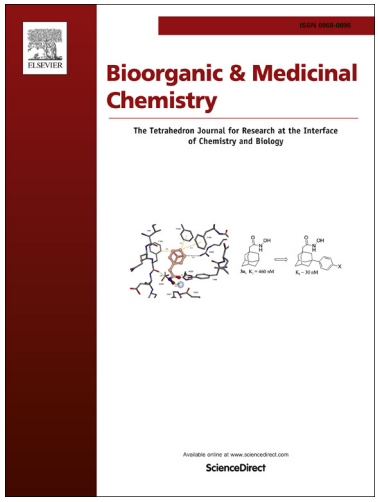

Design, Synthesis, and Biological Evaluation of Scaffold-Based Tripeptidomimetic Antagonists for CXC Chemokine Receptor 4 (CXCR4)

Zack G. Zachariassen, Stefanie Thiele, Erik A. Berg, Pernille Rasmussen, Torgils Fossen, Mette M. Rosenkilde, Jon Våbenø, Bengt Erik Haug

PII: S0968-0896(14)00507-0
DOI: http://dx.doi.org/10.1016/j.bmc.2014.07.004
Reference: BMC 11698

To appear in: *Bioorganic & Medicinal Chemistry*

Received Date: 28 March 2014
Revised Date: 26 June 2014
Accepted Date: 2 July 2014

Please cite this article as: Zachariassen, Z.G., Thiele, S., Berg, E.A., Rasmussen, P., Fossen, T., Rosenkilde, M.M., Våbenø, J., Haug, B.E., Design, Synthesis, and Biological Evaluation of Scaffold-Based Tripeptidomimetic Antagonists for CXC Chemokine Receptor 4 (CXCR4), *Bioorganic & Medicinal Chemistry* (2014), doi: http://dx.doi.org/10.1016/j.bmc.2014.07.004

Design, Synthesis, and Biological Evaluation of Scaffold-Based Tripeptidomimetic Antagonists for CXC Chemokine Receptor 4 (CXCR4)

Zack G. Zachariassen,[a] Stefanie Thiele,[b] Erik A. Berg,[c] Pernille Rasmussen,[c] Torgils Fossen,[c] Mette M. Rosenkilde,[b] Jon Våbenø,*[,a] Bengt Erik Haug*[,c]

[a]*Department of Pharmacy, Faculty of Health Sciences, UiT The Arctic University of Norway, Breivika, NO-9037 Tromsø, Norway.*
[b]*Laboratory for Molecular Pharmacology, Department of Neuroscience and Pharmacology, Faculty of Health and Medical Sciences, University of Copenhagen, Blegdamsvej 3, DK-2200 Copenhagen, Denmark.*
[c] *Department of Chemistry and Centre for Pharmacy, University of Bergen, Allégaten 41, NO-5007 Bergen, Norway.*

Corresponding author for the review process:
Bengt Erik Haug. Phone: +47 55 58 34 68; e-mail: Bengt-Erik.Haug@farm.uib.no

Post-publication corresponding authors:
*Bengt Erik Haug. Phone: +47 55 58 34 68; e-mail: Bengt-Erik.Haug@farm.uib.no
or
*Jon Våbenø. Phone: +47 77 62 09 09; e-mail: jon.vabeno@uit.no

Notes:
The authors declare no competing financial interest.

Keywords:
CXCR4 antagonist, cyclopentapeptide, peptidomimetic, scaffold

Abstract

Structure-activity relationship studies of the cyclopentapeptide CXCR4 antagonists (cyclo(-L-/D-Arg^1-Arg^2-2-Nal^3-Gly^4-D-Tyr^5-)) suggest that the L-/D-Arg^1-Arg^2-2-Nal^3 tripeptide sequence contained within these cyclopentapeptides serves as a recognition motif for peptidic CXCR4 antagonists. Starting by dissecting the cyclopentapeptide structure and reintroducing cyclic constraints in a stepwise manner, we here report a novel class of scaffold-based tripeptidomimetic CXCR4 antagonists based on the D-Arg-Arg-2-Nal motif. Biological testing of the prototype compounds showed that they represent new peptidomimetic hits; importantly, the modular nature of the scaffold provides an interesting starting point for future ligand optimization.

Graphical Abstract

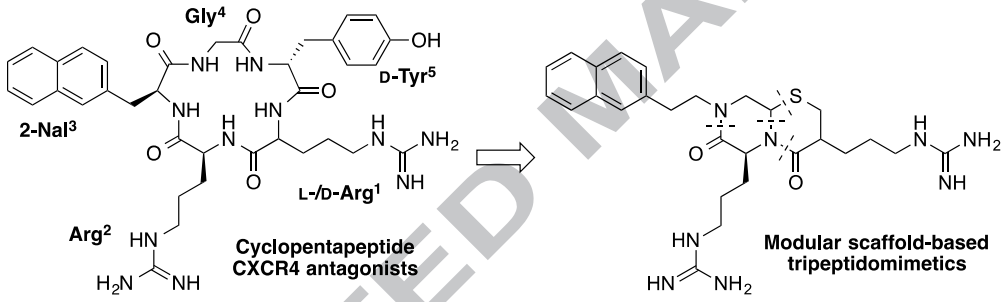

1. INTRODUCTION

CXC chemokine receptor 4 (CXCR4) is a peptidergic GPCR with the 68-residue peptide CXC chemokine ligand 12 (CXCL12) as its only endogenous ligand.[1,2] In addition to the developmental and physiological role of CXCL12/CXCR4, CXCR4 has been shown to be involved in a number of pathological conditions, including HIV, cancer, and rheumatoid arthritis.[3] Consequently, CXCR4 has emerged as an attractive drug target, and several small-molecule CXCR4 antagonists have been described in the literature over the last decade,[3,4] including a series of cyclic pentapeptides based on the amino acid sequence L-/D-Arg^1-Arg^2-2-Nal^3-Gly^4-D-Tyr^5 (2-Nal = L-3-(2-naphthyl)alanine), i.e. the L-Arg^1 epimer **1** (FC131) and the D-Arg^1 epimer **2** (FC092) (Figure 1).[5]

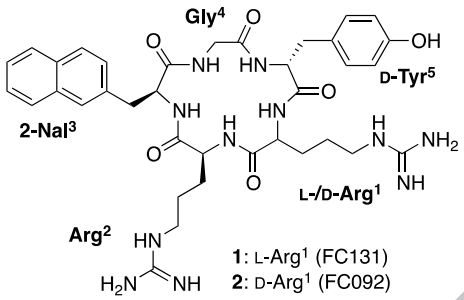

Figure 1. Structures of the lead cyclopentapeptide antagonists **1** and **2**.

Small cyclic peptides, such as cyclopentapeptides, are known to mimic peptide turns,[6] i.e. structural motifs where the peptide backbone folds back on itself to form a pseudo-cyclic structure. Such turns appear to be a universal ligand recognition element for peptidergic GPCRs;[7] thus, the cyclopentapeptide CXCR4 antagonists represent an excellent starting point for design of novel CXCR4 antagonists based on smaller turn-mimicking scaffolds. Such scaffolds have to maintain the 3D-orientation of the pharmacophoric groups of the parent peptide, resulting in a so-called topographical (or type-III) peptidomimetic.[8] With respect to size, a recent review points out that three amino acids represent an optimal size for small-molecule peptidomimetics.[9]

The Gly^4 residue in the cyclopentapeptide CXCR4 antagonists (Figure 1) was originally introduced for synthetic reasons[5] and thus can be considered as a spacer. Through SAR studies, it has become clear that the D-Tyr^5 side chain is not essential for biological activity,[10,11] and we have in a recent molecular docking study found that this may stem from the lack of a defined binding pocket for the D-Tyr^5 side chain.[11] Even if our modeling

suggested that D-Tyr^5 of **1** is partly solvent exposed, the phenolic hydroxyl group was found to take part in hydrogen bonding to Glu^{32}.[11] However, as the D-Phe^5 analogue was found to be only 2-fold less potent, this H-bond is not essential for antagonistic activity; indeed, the Gly^5 analogue of **1** was found to be only one order of magnitude less potent than **1** in our assay system.[11] Collectively, these observations imply that the remaining L-/D-Arg^1-Arg^2-2-Nal^3 tripeptide fragment serves as a recognition motif for peptidic CXCR4 antagonists, which motivates further studies of both flexible and constrained small molecules containing this motif. Through dissection of the cyclopentapeptide structure and a stepwise reintroduction of cyclic constraints, we here report the design, synthesis, and biological evaluation of a novel class of scaffold-based tripeptidomimetic CXCR4 antagonists based on the D-Arg-Arg-2-Nal motif.

2. RESULTS AND DISCUSSION

2.1. General Design Considerations.

As SAR studies of the cyclopentapeptide CXCR4 antagonists (Figure 1) have demonstrated that position 2 (L-Arg) is very sensitive to structural modifications,[12,13] we decided to keep L-Arg^2 throughout this study. Similarly, we have recently shown that replacement of L-2-Nal in position 3 with aromatic/alicyclic analogs results in significant reduction of the antagonistic potency,[11] and therefore used a 2-naphthyl group with the appropriate spacer length for all compounds. In contrast, position 1 has been shown to be relatively tolerant to structural modifications, both with respect to stereochemistry (L- or D-arginine) and the chemical nature of the side chain.[13,14] Even if the originally discovered L-Arg^1 epimer **1** displays somewhat higher affinity than the D-Arg^1 epimer **2** (Figure 1; IC_{50}-values of 0.004 and 0.008 μM, respectively),[5] subsequent SAR studies have shown that cyclopentapeptide analogs containing D-Arg^1 in many cases are more active than the corresponding L-Arg^1 epimers. For example, the most active cyclopentapeptide CXCR4 antagonist reported to date is the N-methylated D-Arg^1 epimer FC122 (cyclo(-N-Me-D-Arg^1-Arg^2-2-Nal^3-Gly^4-D-Tyr^5-)), which showed 8-fold higher affinity than the corresponding L-Arg^1 epimer (IC_{50}-values of 0.003 and 0.023 μM, respectively).[10] Moreover, head-to-tail cyclization of peptides is known to be facilitated by incorporation of a D-amino acid in an all-L sequence due to a turn-inducing effect.[15] For these reasons, we decided to focus on the D-Arg^1 epimers in the present study, using the lead cyclopentapeptide **2** (cyclo(-D-Arg^1-Arg^2-2-Nal^3-Gly^4-D-Tyr^5-), Figure 2A) as starting point.

2.2. Biological Evaluation.

The antagonistic potency of the synthesized compounds **2**–**14** (Figures 2 and 6) on human CXCR4 was determined by a functional assay as previously described[13] and is shown in Table 1; the EC_{50}-value of the known lead compound **2** was 0.52 μM.

Table 1. Antagonistic potency of compounds **2**–**14** on human CXCR4.

Compd[a]	**log EC_{50} ± SEM**[b]	**EC_{50} (μM)**
2[c]	-6.28 ± 0.09	0.52
3	-4.24 ± 0.35	58
4	-4.07 ± 0.24	86
5	-4.36 ± 0.10	44
6	> -4	>100
7	> -4	>100
8	> -4	>100
9	> -4	>100
10	-4.22 ± 0.06	60
11	> -4	>100
12	> -4	>100
13	-4.10 ± 0.31	80
14	-4.20 ± 0.12	64

[a]For structures, see Figures 2 and 6.

[b]Values represent the mean of at least three independent experiments performed in duplicates.

[c]Known compound.[5]

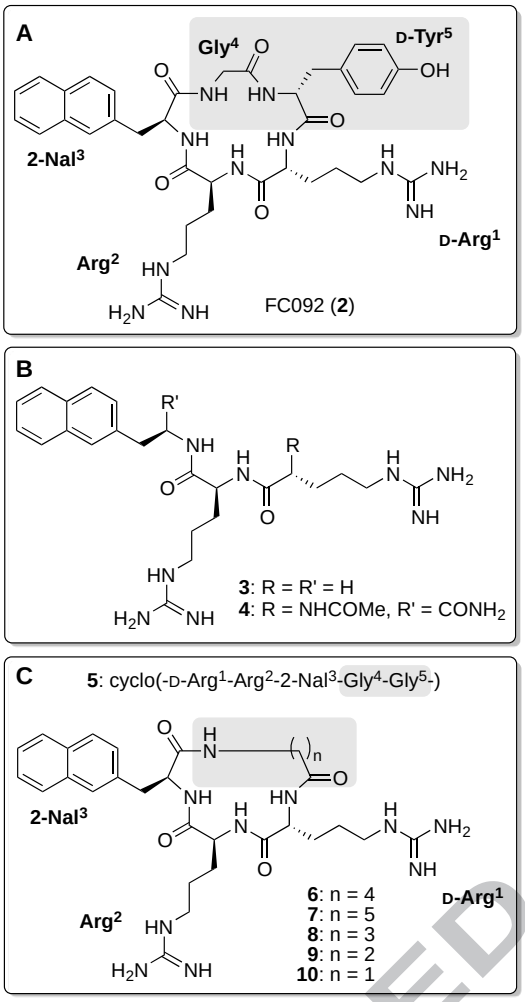

Figure 2. Structures of (A) the lead cyclopentapeptide **2**, (B) the tripeptidic compounds **3**–**4**, and (C) the macrocyclic compounds **5**–**10**.

2.3. Design and SAR.

2.3.1. Linear Tripeptidic Compounds.

Taking a minimalist approach, **2** was initially dissected to the linear peptidic derivative **3** (Figure 2B) in order to determine the activity of the isolated Arg^1-Arg^2-2-Nal^3 motif. The *N*-acetylated D-Arg^1-Arg^2-2-Nal^3 tripeptide amide **4** (Figure 2B) was also included to study the role of the two flanking amide groups. Compound **3** (EC_{50} = 58 μM) displayed 112-fold lower potency than **2**, reflecting the extensive dissection of the cyclopentapeptide structure. This finding is consistent with literature data for similar linear tripeptidic CXCR4 antagonists originating from an Arg-Arg-Nal motif;[16,17] representative structures are shown in Figure 3. In the same way as **3**, these compounds were based on a central L-arginine, and were found to have moderate potency (anti-HIV assay), typically in the order of 100-fold reduction relative to the parent cyclopentapeptide.

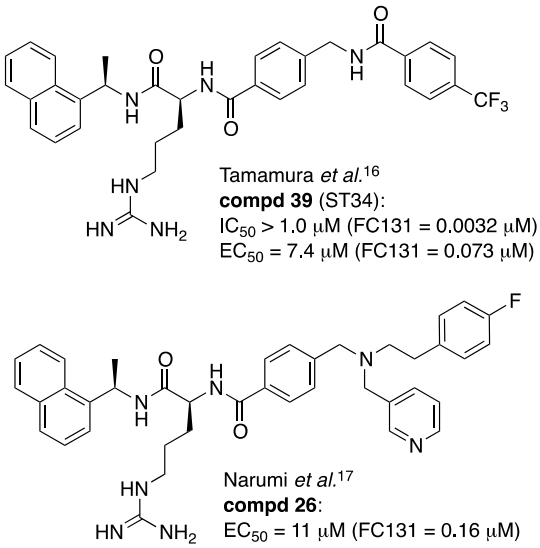

Figure 3. Structures of previously reported linear tripeptidic CXCR4 antagonists.[16,17]

The N- and C-terminal capped linear tripeptide **4** showed somewhat lower activity (EC_{50} = 86 μM) than **3**; thus, the terminal amide groups of **4** do not contribute favorably to activity. The activity of **4** relative to **2** (165-fold reduction) is consistent with SAR studies by Fujii *et al.* which showed that the linear N- and C-terminal capped pentapeptide Ac-D-Arg^1-L-Arg^2-L-2-Nal^3-Gly^4-D-Tyr^5-NH_2 was 173-fold less potent (anti-HIV assay) than the parent cyclopentapeptide **2**.[5]

2.3.2. Macrocyclic Compounds.

The analogs **3** and **4** are quite flexible, which is generally considered as an undesirable feature, and a macrocyclic constraint was reintroduced to force the D-Arg^1-Arg^2-2-Nal^3 motif into a more restricted conformation (Figure 2C). Use of a Gly^4-Gly^5 dipeptide spacer to give a simplified cyclopentapeptide (**5**) resulted in a slight increase in potency (EC_{50} = 44 μM) relative to **4**. Since the Gly^4-Xaa^5 amide bond was not found to be involved in direct binding interactions with the receptor in our recently proposed binding mode,[11] **5** was further simplified by replacing Gly^4-Gly^5 with a 5-aminopentanoic $acid^4$ hydrocarbon spacer (**6**). This modification, which essentially is an ethylene amide bond isostere ($\Psi[CH_2CH_2]$) replacement, resulted in loss of activity in our assay (EC_{50} > 100 μM). This shows that the planar and polar Gly^4-Gly^5 amide bond in **5** contributes favorably to activity, either by geometrical or solvation effects.

Next, we employed a ring expansion/contraction strategy by using ω-amino carboxylic acid spacers of different length (**7**–**10**, Figure 2C). Extension of the hydrocarbon spacer in **6** (15-membered ring) to give a 16-membered ring (**7**) or contraction to give a 14-membered ring (**8**) did still not give any measurable activity (EC_{50} > 100 μM for both compounds). Similarly, the 13-membered ring (**9**) was inactive (EC_{50} > 100 μM); however, the further constrained cyclotetrapeptide **10** (12-membered ring) was equipotent (EC_{50} = 60 μM) with the linear tripeptidic compound **3**.

2.3.3. Bicyclic Tripeptidomimetics.

Encouraged by the activity of **10**, we set out to develop a further constrained turn-mimicking scaffold capable of presenting the side chains and backbone of the D-Arg^1-Arg^2-2-Nal^3 fragment of the cyclopentapeptide **2** in the required 3D-orientation. The key to successful development of such topographical peptidomimetics is knowledge of the bioactive conformation of the parent peptide, in this case the cyclopentapeptide ligands. Based on an extensive exploration of the conformational space for a series of cyclopentapeptide CXCR4 antagonists from the literature, we have previously reported a 3D pharmacophore model that describes the spatial arrangement of the pharmacophoric side chains as well as the bioactive conformation of the cyclopentapeptide backbone.[18]

Searching through the extensive literature on turn-mimetics (see ref [19] for a review), we were intrigued by the tripeptide-derived 3,6,8-trisubstituted[20] bicyclic structure **A** (Figure 4A),[21,22] which contains two endocyclic amide bonds. The synthesis of **A** was first reported by Vojkovsky *et al.* who suggested it as a potential peptide-turn motif;[21] however, no biological applications of **A** have yet been reported. In order to elucidate whether this scaffold would be suitable for our purpose, a structural comparison of low-energy conformations of **A** with our 3D pharmacophore model was undertaken. This showed that scaffold **A** is able to orient the side chains in a similar way as the parent cyclopentapeptide (Figure 4B).

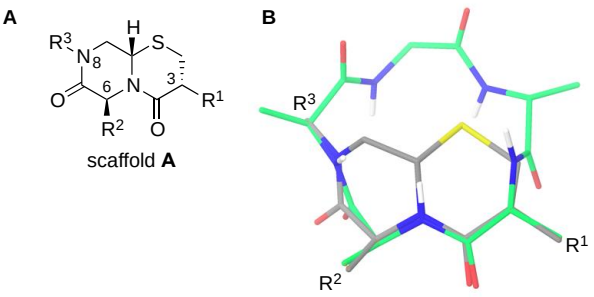

Figure 4. (A) Structure of scaffold **A**, and (B) superimposition of a low-energy conformation of **A** (grey carbon atoms) and the bioactive backbone conformation of the cyclopentapeptide CXCR4 antagonists (green carbon atoms) as defined by our 3D pharmacophore model.[18] RMSD = 0.160 Å (cf. section 4.2).

Scaffold **A** contains three stereocenters, where two (C3 and C6) are defined by the building blocks (see Scheme 4 in Chemistry section). The bridge-head stereocenter (C9a) is formed in the final cyclization step, and the stereochemical outcome has been shown to be governed by the configuration at C3 (see Chemistry section);[23] thus, two diastereomeric scaffolds **A** and **A'** (Figure 5A) can be prepared. Interestingly, structural comparison of the expected bioactive conformation of **A** (shown in Figure 4B) with low-energy conformations of **A'** showed that **A'** can adopt an almost identical conformation with respect to the orientation of the two amide bonds and the three side chains (Figure 5B).

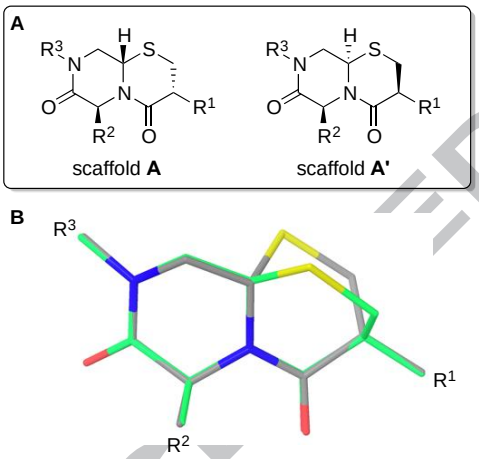

Figure 5. (A) Structures of the diastereomeric scaffolds **A** and **A'**, and (B) superimposition of low-energy conformations of **A** (grey carbon atoms) and **A'** (green carbon atoms). RMSD = 0.036 Å (cf. section 4.2).

Thus, we decided to pursue tripeptidomimetic compounds **11** and **12** (based on scaffold **A** and **A'**, respectively; Figure 6) by using L- and D-cysteine as building blocks, resulting in an amide group in the R^1 side chain. In order to introduce the same arginine R^1 side chain as the parent cyclopentapeptide, we also adapted the synthesis to allow for preparation of **13** and **14** (Figure 6), which in contrast to **11** and **12** do not carry this amide bond.

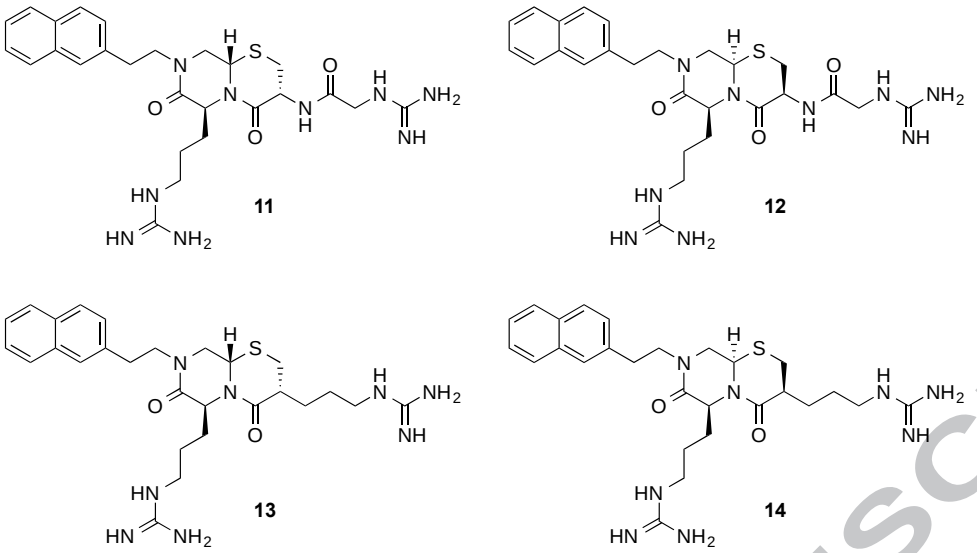

Figure 6. Structures of the bicyclic target compounds **11**–**14**.

Interestingly, compounds **11** and **12** were inactive, while compounds **13** and **14** (EC_{50} = 80 and 64 μM, respectively) showed activity similar to **3** and **10**. Clearly, the amide bond in the R^1 side-chain of **11** and **12** is unfavorable for the biological activity, an observation that justifies the synthetic effort put into the R^1 building block **33** that was used for **13** and **14** (see Scheme 7, Chemistry section). Thus, **13** and **14** represent new peptidomimetic hit compounds for CXCR4 antagonism.

The scaffold-based tripeptidomimetics **13** and **14** are significantly less potent (154- and 123-fold, respectively) than the optimized cyclopentapeptide **2** that they are based on. This was an expected consequence of the rather extensive structural changes that were needed in order to arrive at downsized structures. To our knowledge, there are only two other examples of scaffold-based tripeptidomimetic CXCR4 antagonists in the literature (Figure 7): Niida *et al.* used a 1,3,6-trisubstituted 1,6-dihydropyridin-2-one scaffold,[24] while Ueda *et al.* have reported a series of achiral CXCR4 antagonists based on a 1,2,5-trisubstituted indole scaffold.[25] Also for these compounds, a significant drop in activity compared to the parent cyclopentapeptides was observed; the same group has typically reported an IC_{50}-value of 0.008 μM for the cyclopentapeptide **2**, which means that the affinity reduction for the dihydropyridin-2-one based compound (IC_{50} = 15.1 μM) and the indole-based compound (IC_{50} = 3.0 μM) was 1888- and 375-fold, respectively. These numbers reflect the general complexity of the initial "scaffold jump" for prototype compounds, as also seen in the present study.

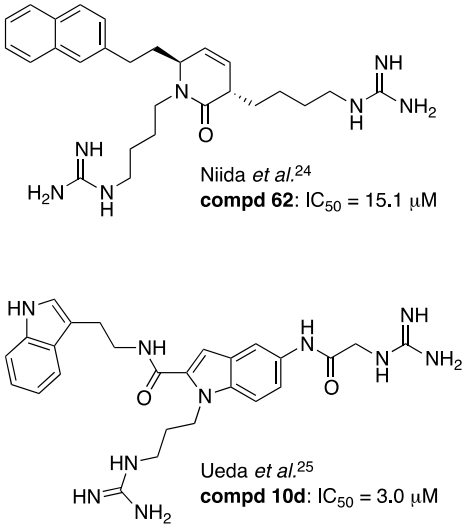

Figure 7. Structures of previously reported scaffold-based tripeptidomimetic CXCR4 antagonists.[24,25]

The moderate activity of our prototype bicyclic tripeptidomimetics **13** and **14** also means that binding mode studies (typically performed by combining site-directed receptor mutagenesis studies and molecular docking) are not expected to provide reliable data for these compounds. Thus, further SAR studies, aimed at optimizing both the scaffold core and the side chains, are currently in progress.

2.4. Chemistry.

The macrocyclic compounds **2** and **5**–**10** were prepared by head-to-tail macrolactamization of linear precursors (Scheme 1) that were obtained through Fmoc-based solid phase peptide synthesis (SPPS). The linear precursors were prepared using either a preloaded Fmoc-Gly trityl resin (**2**, **5**, and **10**) or a 2-chlorotrityl chloride resin for the loading of the N-Fmoc ω-aminocarboxylic acids (**6**–**9**). Cleavage from the resin was facilitated using hexafluoroisopropanol and the side-chain protected peptides were cyclized using PyBOP followed by global deprotection using TFA.

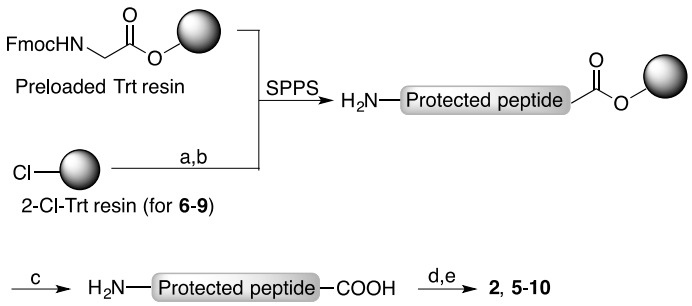

Scheme 1. Synthesis of **2** and **5**–**10**. *Reagents and conditions:* (a) N-Fmoc ω-amino-carboxylic acid, DIPEA, CH_2Cl_2, rt, 1 h; (b) MeOH, DIPEA, CH_2Cl_2, rt, 2 x 5 min (c) HFIP, CH_2Cl_2, rt, 15 min, then 2 x 10 min; (d) PyBOP, DIPEA, DMF/CH_2Cl_2, rt, 24 h; (e) TFA/TIS/H_2O, rt, 2 h.

Compound **3** was synthesized (Scheme 2) by coupling protected arginine **15** with 2-(naphthalene-2-yl)ethanamine to give **16**, which in turn was Fmoc-deprotected and coupled with N-Boc 5-aminopentanoic acid to give **17**. Global deprotection facilitated by TFA followed by guanidinylation of the primary amine gave **3**.

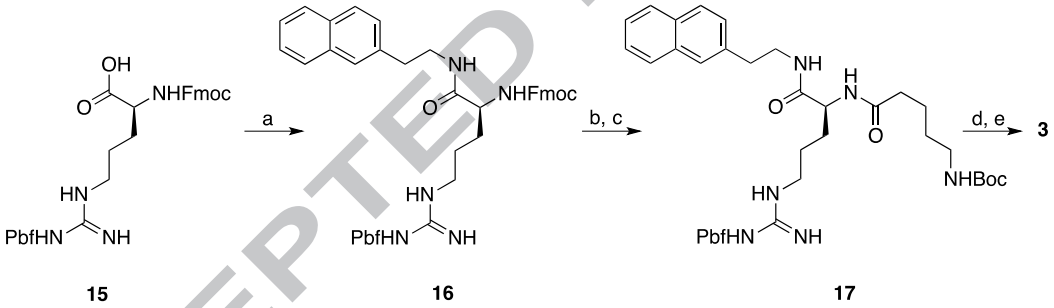

Scheme 2. Synthesis of **3**. *Reagents and conditions:* (a) 2-(naphthalene-2-yl)ethanamine hydrochloride, HBTU, DIPEA, DMF, rt, 20 h; (67%); (b) 2-ethanolamine, DMF, rt, 3 h; (c) *N*-Boc 5-aminopentanoic acid, HATU, DIPEA, DMF, 24 h; (d) TFA/TIS/H_2O, rt, 2 h; (e) 1*H*-pyrazole-1-carboxamidine hydrochloride, DIPEA, DMF, rt, 48 h (21% over four steps).

The linear tripeptide **4** was prepared by Fmoc-based SPPS on an Fmoc-NH-Rink amide resin (Scheme 3) followed by acetylation of the N-terminal using acetic anhydride. Cleavage from the resin and global deprotection mediated by TFA gave the desired N-acetylated tripeptide amide **4**.

Scheme 3. Synthesis of **4**. *Reagents and conditions:* (a) Ac_2O, DIPEA, DMF, rt, 30 min; (b) TFA/TIS/H_2O, rt, 3 h.

The key step in the synthesis of the bicyclic tripeptidomimetics **11**–**14** (Scheme 4) is the spontaneous formation of the 6,6-fused bicyclic ring system **A** upon treatment of acetal **C** with TFA.[21,22] The resulting aldehyde condensates with the backbone amide nitrogen to give the *N*-acyliminium ion intermediate **B**, which subsequently undergoes nucleophilic attack from the deprotected thiol, resulting in the formation of the desired bicycle **A**.[21,22] The cyclization occurs stereoselectively,[23] and the configuration at the bridge-head (C9a) is dependent on the configuration at C3 (R^1 substituent), and in the absence of a R^1 substituent on the configuration at C6.

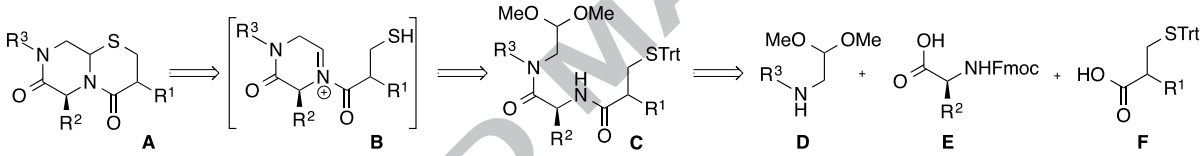

Scheme 4. Scaffold and retrosynthetic strategy.

Synthesis of the linear precursor **C** requires access to the three building blocks **D**, **E** and **F**. For the synthesis of target compounds **11** and **12**, the R^1-side chain (incorporated through building block **F**) was introduced as guanidinylated glycine **20** (Scheme 5). This material was prepared by guanidinylation of glycine methyl ester hydrochloride (**18**) using *N*,*N*-di-Boc-1*H*-pyrazole-1-carboxamidine followed by hydrolysis of the methyl ester of the resulting **19** using LiOH in a mixture of water and acetone.[26,27]

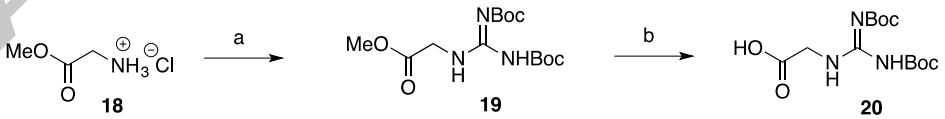

Scheme 5. Synthesis of carboxylic acid **20**. *Reagents and conditions:* (a) *N*,*N*-di-Boc-1*H*-pyrazole-1-carboxamidine, DIPEA, DMF, rt, 14 h (85%); (b) LiOH, H_2O/acetone, rt, 1.5 h (99%).

Synthesis of the bicyclic core (Scheme 6) commenced with the alkylation of 2-(naphthalene-2-yl)ethanamine (**21**) with bromoacetaldehyde dimethyl acetal in refluxing THF to give

secondary amine **22**. This amine was in turn coupled with protected arginine (**15**) to give **23** in high yield. Further Fmoc-deprotection and coupling with appropriately protected L-cysteine gave **24**, which was submitted to another Fmoc-deprotection and then coupled with carboxylic acid **20** to give the linear precursor **25**. This material was treated with TFA, thioanisole and water to facilitate global deprotection, leading to formation of the acyliminium ion intermediate that after nucleophilic attack by the thiol gave **11**. The diastereomeric **12** was prepared by coupling of Fmoc-D-Cys(Trt)-OH to Fmoc-deprotected **23** to give intermediate **26** (see Experimental section), which in turn was converted to linear precursor **27** followed by deprotection and cyclization to give **12**.

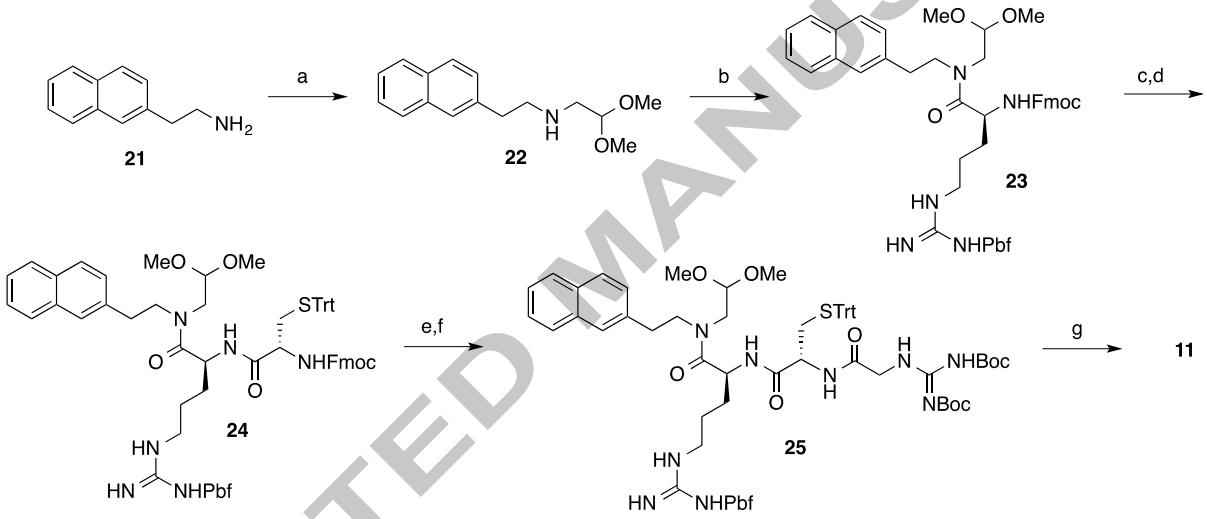

Scheme 6. Synthesis of the bicyclic tripeptidomimetic **11**. *Reagents and conditions:* (a) $BrCH_2CH(OMe)_2$, THF, reflux, 24 h (30%); (b) Fmoc-Arg(Pbf)-OH (**15**), HATU, DIPEA, DMF, rt, 16 h (83%); (c) Et_2HN, CH_2Cl_2, rt, 2 h; (d) Fmoc-L-Cys(Trt)-OH, HATU, DIPEA, CH_2Cl_2, rt, 22 h (49% over two steps); (e) Et_2HN, CH_2Cl_2, rt, 2 h; (f) **20**, HATU, DIPEA, CH_2Cl_2, rt, 18 h (57% over two steps); (g) TFA/thianisole/H_2O, rt, 2.5 h (13% after HPLC purification).

The configuration of the newly formed stereocenters at the bridge-head carbon atoms (C9a) in **11** and **12** (see Figure 5) was determined using the 2D ^{1}H ROESY experiment (see supplementary data for detailed ROESY spectra for **11** and **12**). The known configurations of C6 (*S* for both **11** and **12**) and C3 (*R* for **11** and *S* for **12**) were used as prerequisites for determination of the configuration of C9a. The strong cross-peaks observed at δ 5.09/4.71 (H9a/H3), δ 5.09/1.73 (H9a/Hβ arginine R^2) and the medium strong cross-peak at δ 5.09/1.44 (H9a/Hγ arginine R^2) observed in the 2D ROESY spectrum of **11** confirmed the (*S*)

configuration of C9a in **11**. Moreover, the strong cross-peak observed at δ 5.00/4.72 (H9a/H3) in the 2D ROESY spectrum of **12** and the presence of only very weak cross-peaks at δ 5.00/1.64 (H9a/Hβa arginine R^2) and δ 5.00/1.52 (H9a/Hβb arginine R^2) confirmed the (*R*) configuration of C9a in **12**.

The **F** building block required for **13** and **14** required a multi-step synthesis (Scheme 7). 2-Oxopiperidine derivative **28** was selectively reduced using freshly prepared $Ca(BH_4)_2$, and after an acidic work-up, alcohol **29** was isolated in good yield.[28] The alcohol was next taken through a carbodiimide-mediated dehydration to give α,β-unsaturated lactam **30**.[28] Use of *N*-(3-dimethylaminopropyl)-*N*′-ethylcarbodiimide (EDC) in refluxing toluene gave up to 73% yield, while DCC gave the product in quantitative yield. In both cases, CuI was added to activate the carbodiimide. Next, the lactam was Boc-protected to give **31** followed by Michael addition of triphenylmethane thiol to give racemic **32**, with excellent yield in both steps. Finally, the Boc-protected lactam was hydrolyzed using LiOH to give racemic carboxylic acid **33** in high yield.

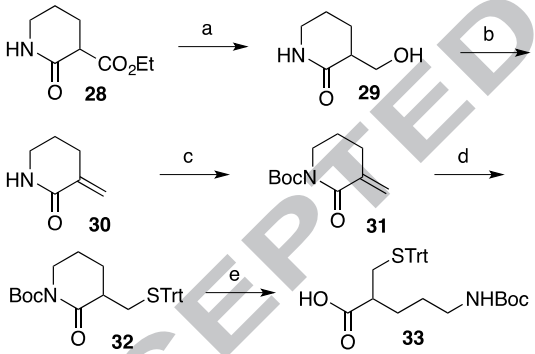

Scheme 7. Synthesis of building block **33**. *Reagents and conditions.* (a) $CaCl_2$, $NaBH_4$, MeOH, 0 °C, 2 h, then rt, 16 h (76%); (b) DCC, CuI, toluene, 110 °C, 1 h (quant); (c) Boc_2O, Et_3N, DMAP, CH_2Cl_2/DMF, rt, 14 h (94%); (d) Ph_3CSH, Et_3N, CH_2Cl_2, rt, 14 h (95%); (e) 1M aq. LiOH, THF, rt, 1 h (94%).

Assembly of the linear precursors for **13** and **14** (Scheme 8) was carried out by Fmoc-deprotecting **23** and subsequent coupling of the resulting material with carboxylic acid **33**, to give **34** as an inseparable mixture of diastereoisomers. Linear precursor **34** was globally deprotected and cyclized, and the amino group was guanidinylated to give **13** and **14**.

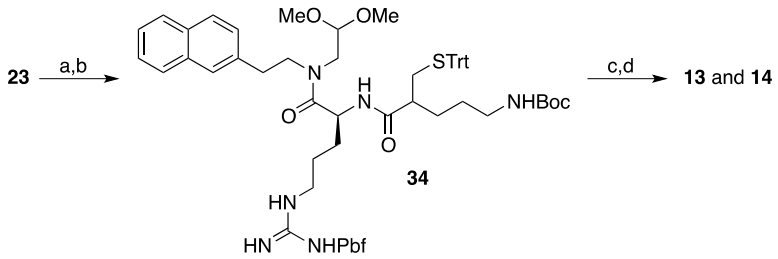

Scheme 8. Synthesis of **13** and **14**. *Reagents and conditions.* (a) Et_2HN, CH_2Cl_2, rt, 3 h; (b) **33**, HBTU, DIPEA, CH_2Cl_2, rt, 17 h (85% over two steps); (c) TFA/thioanisole/H_2O, rt, 1.5 h; (d) 1*H*-pyrazole-1-carboxamidine hydrochloride, DIPEA, DMF, rt, 72 h (7% for **13**, 11% for **14**, over two steps and after HPLC purification).

RP-HPLC analysis after guanidinylation showed two distinct peaks, which were separable by semi-prep RP-HPLC. NMR analysis of the two isolated products clearly showed that they were single diastereoisomers. For the two isolated products, only the configuration at C6 (*S*) was known, and the configuration of C3 and C9a was determined using the 2D ^{1}H ROESY experiment (see supplementary data). For both **13** and **14**, strong cross-peaks between H9a and H3 (at δ 5.14/2.74 and at δ 4.66/2.38 for **13** and **14**, respectively) were observed, indicating similar overall geometry to that of **11** and **12**. The presence of a cross-peak between H9a and Hγ arginine R^2 was observed only in the ROESY spectrum of **13** suggesting that the configuration of C9a for this compound is *S*, whereas the configuration of C9a for the stereoisomer **14** is *R*. Since H9a and H3 are *cis* in both **13** and **14**, the configuration at C3, which stems from the racemic carboxylic acid **33**, is *R* in **13** and *S* in **14**. It is interesting to note that *S* configuration of C9a in **11** and **13** leads to a downfield shift of H6 when compared with the analogous *R* isomer. Grimes *et al.* speculated that a solvent mediated hydrogen bond between the R^1-side chain amide NH and the ring carbonyl group could contribute to stabilizing a conformation in which the R^1 substituent is in an equatorial position, which favors the observed stereoselectivity of the cyclization.[23] However, for the formation of **13** and **14**, the absence of a R^1 amide NH did not influence on the stereoselectivity in the cyclization step.

3. CONCLUSIONS

In this work we have demonstrated that new scaffold-based tripeptidomimetic CXCR4 antagonists can be rationally designed from cyclopentapeptide CXCR4 antagonists. The bicyclic compounds reported herein represent an interesting class of new tripeptidomimetic CXCR4 antagonists, and although the prototype compounds showed moderate activity, they

serve as useful leads for further optimization. The peptidomimetic scaffold we have employed is constructed from three building blocks, each containing one of the pharmacophoric groups, and therefore allows for synthetic access to a range of target molecules. We envision that further SAR studies involving the three different binding groups will afford new and optimized CXCR4 antagonists.

4. EXPERIMENTAL SECTION

4.1. Chemistry.

All reagents and starting materials were purchased from Sigma-Aldrich and used as delivered unless otherwise stated. Cyclic peptide **2** was prepared as previously described.[13] The preparation of **4**–**10** is described in the supplementary data. Anhydrous toluene, CH_2Cl_2 and THF were obtained from an anhydrous solvent delivery system (SDS-800 from mBraun) at the Department of Chemistry, University of Bergen. Analyses using thin layer chromatography were performed on Alugram® SIL G/UV_{254} 0.20 mm layer plates from Machery-Nagel or on aluminum sheets with Merck silica gel (60 F_{254}). TLC plates were visualized using either ultraviolet light or by immersing the plate in 2% solution of ninhydrin in ethanol containing 10 drops of concentrated sulphuric acid pr 100 mL followed by heating. Purification by flash column chromatography was performed using J.T Baker Silica Gel or Merck 60 Kieselgel (230-400 mesh). All final compounds were purified using semi-preparative RP-HPLC eluting with mixtures of acetonitrile and H_2O (both containing 0.1% TFA). Fractions of equal purity were pooled and lyophilized. All tested compounds were analyzed by RP-HPLC and found to be of >95% purity (UV 220 nm).

4.1.1. (9*H*-Fluoren-9-yl)methyl (*S*)-(1-((2-(naphthalen-2-yl)ethyl)amino)-1-oxo-5-(3-((2,2,4,6,7-pentamethyl-2,3-dihydrobenzofuran-5-yl)sulfonyl)guanidino)pentan-2-yl)carbamate (16)

HBTU (945 mg, 2.4 mmol) and DIPEA (0.66 mL, 3.7 mmol) were added to a stirred solution of Fmoc-Arg(Pbf)-OH (809 mg, 1.2 mmol) in dry DMF (3 mL) under an argon atmosphere. The mixture was stirred at room temperature for 30 min before a solution of 2-(naphthalen-2-yl)ethan-1-amine hydrochloride (518 mg, 2.5 mmol) in DMF (2 mL) was added drop-wise to the reaction mixture, and stirring continued for 20 h. The solvent was evaporated and the residue was partitioned between EtOAc (20 mL) and H_2O (10 mL). The organic phase was washed with H_2O (2 x 10 mL), 5% $KHCO_3$ (20 mL) and brine (20 mL), dried over $MgSO_4$,

filtered and evaporated. The crude product was purified by flash chromatography on silica gel (EtOAc/hexane; gradient 1:1 to 9:1) to give the title compound as a white solid (706 mg, 67%). R_f (EtOAc/hexane 9:1) = 0.23; ^{1}H NMR (400 MHz, $CDCl_3$) δ = 7.75 – 7.67 (m, 5H), 7.60 – 7.49 (m, 3H), 7.41 – 7.32 (m, 4H), 7.31 – 7.26 (m, 2H), 7.26 – 7.23 (m, 1H), 4.34 – 4.20 (m, 2H), 4.17 – 4.06 (m, 2H), 3.66 – 3.45 (m, 2H), 3.24 – 3.08 (m, 2H), 2.97 – 2.92 (m, 2H), 2.90 – 2.87 (m, 2H), 2.81 – 2.79 (m, 2H), 2.53 (s, 3H), 2.46 (s, 3H), 2.05 (s, 3H), 1.48 – 1.40 (m, 8H); ^{13}C NMR (101 MHz, CD_3OD) δ = 174.9, 173.4, 165.3, 160.3, 158.67, 158.66, 158.4, 145.7, 145.5, 143.0, 143.0, 139.9, 138.3, 135.4, 134.1, 134.0, 129.5, 129.20, 129.18, 129.0, 128.78, 128.74, 128.6, 127.4, 126.8, 126.6, 126.5, 121.3, 118.9, 88.1, 68.2, 62.0, 56.6, 44.3, 42.0, 39.3, 37.4, 36.9, 32.1, 30.9, 29.0, 21.3, 20.0, 18.8, 14.9, 13.0; HRMS (ESI): *m/z* $[M + H]^+$ calcd for $C_{46}H_{52}N_5O_6S$: 802.3633; found: 802.3639.

4.1.2. (*S*)-5-Guanidino-2-(5-guanidinopentanamido)-*N*-(2-(naphthalen-2-yl)ethyl)pentanamide (3)

To a solution of the Fmoc-protected amine **16** (610 mg, 0.77 mmol) in DMF (6 mL) was added 2-ethanolamine (6 mL) and the mixture was stirred for 3 h at room temperature under HPLC monitoring. The solvent was removed in vacuo, the residue was dissolved in EtOAc, washed with H_2O (2 x 10 mL), saturated $NaHCO_3$ (2 x 10 mL) and brine (15 mL). The solvent was evaporated and the crude product (500 mg) was used in the next step without further purification. HRMS (ESI): *m/z* $[M + H]^+$ calcd for $C_{31}H_{41}N_5O_4S$: 580.2952; found: 580.2958.

HATU (590 mg, 1.5 mmol) and DIPEA (0.41 mL, 2.3 mmol) were added to a stirring solution of 5-((*tert*-butoxycarbonyl)amino)pentanoic acid (338 mg, 1.5 mmol) in dry DMF (3 mL) under an argon atmosphere. The mixture was stirred at room temperature for 30 min before a solution of the crude product from the previous step (451 mg, 0.78 mmol) in DMF (1.5 mL) was added drop wise to the reaction mixture, and stirring continued for 24 h. The reaction mixture was partitioned between EtOAc (30 mL) and H_2O (20 mL). The aqueous layer was extracted with EtOAc (2 x 15 mL) and the combined organic layer washed with 10% citric acid (15 mL), 5% $KHCO_3$, (15 mL) and brine (15 mL), and dried over $MgSO_4$. Filtration and removal of the solvent under reduced pressure gave the crude product (520 mg). Purification by flash chromatography (EtOAc/hexane; gradient 1:1 to pure EtOAc, followed by EtOAc/MeOH; gradient 9:1 to 8:2) afforded **17** as colorless foam (358 mg) which was judged to be of sufficient purity for the next step. HRMS (ESI): *m/z* $[M + H]^+$ calcd for $C_{41}H_{59}N_6O_7S$: 779.4160; found: 779.4168.

The Boc-protected amine **17** (358 mg, 0.46 mmol) was dissolved in a mixture of TFA, TIS and H_2O (95:2.5:2.5, 15 mL) and the resulting solution was stirred at room temperature. The reaction was monitored using analytical RP-HPLC and all starting material was found to be consumed after 2 h. The TFA solution was evaporated and the residue was precipitated by addition of cold diethyl ether (10 mL) and cooled overnight. The ether was decanted and the residue was dried *in vacuo* to give the crude product (403 mg), which was used in the next step without further purification. HRMS (ESI): *m/z* $[M + H]^+$ calcd for $C_{23}H_{34}N_6O_2$: 427.2816; found: 427.2816.

To a stirring solution of the crude primary amine (403 mg, 0.61 mmol) in DMF (3 mL) was added 1*H*-pyrazole-1-carboxamidine hydrochloride (453 mg, 3.0 mmol) and DIPEA (0.53 mL, 3.1 mmol) and the resulting mixture was stirred under nitrogen atmosphere for 48 h. The reaction was monitored using analytical RP-HPLC. After the solvent had been evaporated, the residue was precipitated by addition of cold diethyl ether, washed with ether, purified by preparative RP-HPLC, and lyophilized (129 mg, 21% over four steps). ^{1}H NMR (400 MHz, CD_3OD): δ = 7.59 – 7.51 (m, 3H), 7.42 (s, 1H), 7.24 – 7.10 (m, 3H), 4.01 (dd, *J* = 8.3, 5.7, 1H), 3.39 – 3.23 (m, 2H), 2.90 (t, *J* = 6.7, 2H), 2.80 (m, 2H), 2.73 (t, *J* = 7.0, 2H), 2.00 (t, *J* = 7.0, 2H), 1.51 – 1.09 (m, 8H); ^{13}C NMR (101 MHz, CD_3OD): δ = 175.9, 174.3, 158.84, 158.81, 138.0, 135.2, 133.9, 129.3, 128.8, 128.7, 128.54, 128.48, 127.2, 126.6, 54.7, 42.2, 42.0, 41.8, 36.7, 36.1, 30.4, 29.5, 26.4, 23.8; HRMS (ESI): *m/z* $[M + H]^+$ calcd for $C_{24}H_{36}N_8O_2$: 469.3034; found: 469.3033.

4.1.3. Methyl (*N*,*N*'-bis(*tert*-butoxycarbonyl)carbamimidoyl)glycinate (19)[26]

To a slurry of glycine methyl ester hydrochloride (1.11 g, 8.8 mmol) in DMF (30.5 mL) was added *N*,*N*-di-Boc-1*H*-pyrazole-1-carboxamidine (1.02 g, 3.3 mmol) and DIPEA (1.1 mL, 6.3 mmol). The mixture was stirred overnight (14 h) at room temperature and turned into a yellow slurry. The reaction mixture was partitioned between EtOAc (25 mL) and H_2O (20 mL) and the aqueous layer was further extracted three times with EtOAc (25 mL), before the combined organic layers were dried over anhydrous $MgSO_4$. The solvent was evaporated under reduced pressure to give the crude product as a light yellow solid (1.4 g). Further purification using flash column chromatography (Hexanes/EtOAc, 3:1) gave the title compound as a colourless solid (932 mg, 85 %). R_f (Hexanes/EtOAc, 3:1) = 0.27; ^{1}H NMR (400 MHz, $CDCl_3$) δ = 11.44 (s, 1H), 8.87 (s, 1H), 4.25 (d, *J* = 4.9, 2H), 3.78 (s, 3H), 1.51 (s, 9H), 1.50 (s, 9H); ^{13}C NMR (100 MHz, $CDCl_3$) δ = 170.2, 163.6, 156.3, 153.3, 83.7, 79.9,

52.8, 43.0, 28.6, 28.4; HRMS (ESI): *m/z* $[M + H]^+$ calcd for $C_{14}H_{26}N_3O_6$: 332.1822; found: 332.1821.

4.1.4. (*N*,*N*'-bis(*tert*-Butoxycarbonyl)carbamimidoyl)glycine (20)[27]

$LiOH \cdot H_2O$ (166 mg, 4.0 mmol) was added to a solution of methyl ester **19** (330 mg, 1 mmol) in acetone/H_2O (6:1, 4.5 mL) at room temperature. TLC monitoring showed full consumption of the starting material after 1.5 h, and the reaction mixture was cooled to 0 °C before a 0.5 M aqueous HCl solution was added drop-wise until pH 3. The mixture was allowed to warm to room temperature and extracted with EtOAc (3 x 20 mL). Drying over anhydrous Na_2SO_4 and evaporation of the solvent gave the title compound as a colourless solid (312 mg, 99 %). R_f (Hexanes/EtOAc/AcOH, 60:40:1) = 0.20; ^{1}H NMR (400 MHz, $CDCl_3$) δ = 11.37 (s, 1H), 8.87 (s, 1H), 4.18 (s, 2H), 1.51 (s, 9H), 1.49 (s, 9H); ^{13}C NMR (100 MHz, $CDCl_3$) δ = 171.7, 162.2, 157.0, 153.1, 84.4, 80.9, 44.3, 28.5, 28.3; HRMS (ESI): *m/z* $[M + H]^+$ calcd for $C_{13}H_{23}N_3O_6$: 318.1665; found: 318.1657.

4.1.5. 2,2-Dimethoxy-*N*-(2-(naphthalen-2-yl)ethyl)ethan-1-amine (22)

2-(Napthalene-2-yl)ethyl-1-amine (**21**) (322 mg, 1.9 mmol) and bromoacetataldehyde dimethyl acetal (0.2 mL, 1.7 mmol) were dissolved in dry THF (4 mL), and the mixture was heated at a gentle reflux for 24 h. After the solvent was evaporated, the residue was dissolved in CH_2Cl_2 (20 mL) and the organic phase was washed with saturated $NaHCO_3$ (2 x 10 mL) and brine. The mixture was concentrated and purified by flash chromatography on silica gel (EtOAc) to give the title compound (130 mg, 30%) as yellow oil. R_f (EtOAc) = 0.14; ^{1}H NMR (400 MHz, $CDCl_3$): δ = 7.78 (t, *J* = 8.6, 3H), 7.64 (s, 1H), 7.49 – 7.37 (m, 2H), 7.33 (d, *J* = 8.4, 1H), 4.45 (t, *J* = 5.4, 1H), 3.34 (s, 6H), 2.96 (s, 4H), 2.78 (d, *J* = 5.4, 2H); ^{13}C NMR (100 MHz, $CDCl_3$): δ = 137.7, 133.8, 132.4, 128.3, 127.9, 127.7, 127.5, 127.2, 126.2, 125.5, 104.2, 54.2, 51.39, 51.36, 36.8; HRMS (ESI): *m/z* $[M + H]^+$ calcd for $C_{16}H_{22}NO_2$: 260.1645; found: 260.1646.

4.1.6. (9*H*-Fluoren-9-yl)methyl (*S*)-(1-((2,2-dimethoxyethyl)(2-(naphthalen-2-yl)ethyl)amino)-1-oxo-5-(3-((2,2,4,6,7-pentamethyl-2,3-dihydrobenzofuran-5-yl)sulfonyl)guanidino)pentan-2-yl)carbamate (23)

HATU (183 mg, 0.48 mmol) and DIPEA (84 µL, 0.48 mmol) were added to a stirred solution of Fmoc-Arg(Pbf)-OH (292 mg, 0.45 mmol) in dry DMF (1.2 mL) under an argon atmosphere. The mixture was stirred at room temperature for 30 min before amine **22** (125

mg, 0.48 mmol) in DMF (0.6 mL) was added drop-wise to the reaction mixture, and stirring continued for 16 h. The reaction mixture was partitioned between H_2O (10 mL) and EtOAc (20 mL). The organic phase was further washed with H_2O (2 x 10 mL) and brine (2 x 10 mL), dried over $MgSO_4$, filtered and evaporated. The crude product was purified by flash chromatography on silica gel (EtOAc/hexane 8.5:1.5) to give the title compound as white foam (334 mg, 83 %, retains EtOAc). R_f (EtOAc/hexane 8.5:1.5) = 0.28; ^{1}H NMR and ^{13}C NMR gave no useful information due to rotamers; HRMS (ESI): *m/z* $[M + H]^+$ calcd for $C_{50}H_{60}N_5O_8S$: 890.4157; found: 890.4166; *m/z* $[M + Na]^+$ calcd for $C_{50}H_{59}N_5O_8SNa$: 912.3977; found: 912.3976.

4.1.7. (9*H*-Fluoren-9-yl)methyl ((7*S*,10*R*)-3-methoxy-5-(2-(naphthalen-2-yl)ethyl)-6,9-dioxo-7-(3-(3-((2,2,4,6,7-pentamethyl-2,3-dihydrobenzofuran-5-yl)sulfonyl)guanidino)propyl)-13,13,13-triphenyl-2-oxa-12-thia-5,8-diazatridecan-10-yl)carbamate (24)

Et_2NH (1.5 mL) was added to a solution of the Fmoc-protected amine **23** (261 mg, 0.29 mmol) in CH_2Cl_2 (3 mL) and the mixture was stirred at room temperature for 2 h with TLC monitoring. The solvent was removed under reduced pressure, to give a light yellow foam. The crude product (230 mg) was used directly in the next step.

To a solution of crude Fmoc-deprotected **23** (0.29 mmol) in CH_2Cl_2 (2 mL), were added Fmoc-Cys(Trt)-OH (183 mg, 0.31 mmol), HATU (112 mg, 0.30 mmol) and DIPEA (0.14 mL, 0.8 mmol), and the mixture was stirred for 22 h at room temperature. After evaporation of the solvent, the residue was partitioned between EtOAc (15 mL) and H_2O (50 mL). The aqueous layer was extracted with EtOAc (2 x 15 mL), and the combined organic layer was washed with 1M $KHSO_4$ (30 mL), H_2O (30 mL), saturated $NaHCO_3$ (30 mL), brine (30 mL) and was dried over anhydrous $MgSO_4$. Removal of the solvent under reduced pressure gave the crude product as an orange colored foam (419 mg). Purification by flash column chromatography (EtOAc/hexanes, 8:2) gave **24** as a colorless foam (194 mg, 49 % over 2 steps). ^{1}H NMR showed that the product retained EtOAc, and the yield is adjusted accordingly. R_f (EtOAc/hexane, 8:2) = 0.16; ^{1}H NMR and ^{13}C NMR gave no useful information due to rotamers; HRMS (ESI): *m/z* $[M + Na]^+$ calcd for $C_{72}H_{78}N_6O_9S_2Na$: 1257.5169; found: 1257.5172.

4.1.8. *tert*-Butyl ((7*S*,10*R*)-3-methoxy-19,19-dimethyl-5-(2-(naphthalen-2-yl)ethyl)-6,9,12,17-tetraoxo-7-(3-(3-(2,2,4,6,7-pentamethyl-2,3-dihydrobenzofuran-5-

ylsulfonyl)guanidino)-propyl)-10-(tritylthiomethyl)-2,18-dioxa-5,8,11,14,16-pentaazaicosan-15-ylidene)carbamate (25)

Et_2NH (0.73 mL) was added to a solution of the Fmoc-protected amine **24** (181 mg, 0.15 mmol) in CH_2Cl_2 (1.5 mL) at room temperature. TLC monitoring showed no sign of the starting material after 2 h and the solvent was removed under reduced pressure to give a light yellow foam. The crude product (183 mg) was used directly in the next step. HRMS (ESI): *m/z* $[M + H]^+$ calcd for $C_{57}H_{69}N_6O_7S_2$: 1013.4669; found: 1013.4672.

To a solution of carboxylic acid **20** (183 g, 0.31 mmol) in CH_2Cl_2 (1 mL), were added HATU (60 mg, 0.16 mmol), DIPEA (0.07 mL, 0.40 mmol) and Fmoc-deprotected **24** (65 mg, 0.2 mmol) and the resulting yellow reaction mixture was allowed to stir for 18 h at room temperature. The solvent was evaporated and the residue was partitioned between EtOAc (10 mL) and H_2O (10 mL). The aqueous layer was extracted with EtOAc (2 x 10 mL), and the combined organic layer was washed with 1M $KHSO_4$ (20 mL), H_2O (20 mL), saturated $NaHCO_3$ (20 mL), brine (20 mL) and was dried over anhydrous $MgSO_4$. Removal of the solvent under reduced pressure gave the crude product as a yellow foam (203 mg). Purification by flash column chromatography (EtOAc/hexanes, 9:1) gave the title compound as a light yellow foam (101 mg, 57 % over 2 steps). ^1H NMR showed that the product retained EtOAc, and the yield is adjusted accordingly. R_f (EtOAc/hexanes, 9:1) = 0.21; ^1H NMR and ^{13}C NMR gave no useful information due to rotamers; HRMS (ESI): *m/z* $[M + H]^+$ calcd for $C_{70}H_{90}N_9O_{12}S_2$: 1312.6145; found: 1312.6146.

4.1.9. 2-Guanidino-*N*-((3*R*,6*S*,9a*S*)-6-(3-guanidinopropyl)-8-(2-(naphthalen-2-yl)ethyl)-4,7-dioxohexahydro-2*H*,6*H*-pyrazino[2,1-*b*][1,3]thiazin-3-yl)acetamide (11)

Linear precursor **25** (92 mg, 0.07 mmol) was dissolved in a mixture of TFA, thioanisole and distilled H_2O (90:5:5, 8 mL) and stirred for 2.5 h at room temperature. After evaporation of the solvent under reduced pressure the brown residue was cooled to 0 °C. Addition of cold ether resulted in precipitation and the crude solid was purified by preparative RP-HPLC, and lyophilized to give **11** as a fluffy white solid (7.2 mg, 13%). ^1H NMR (600 MHz, CD_3OD): δ = 7.82 – 7.79 (m, 3H), 7.70 (s, 1H), 7.47 – 7.41 (m, 3H), 5.09 (dd, *J* = 7.4, 4.0, 1H), 4.95 (dd, *J* = 9.3, 6.1, 1H), 4.71 (t, *J* = 8.8, 1H), 4.03 – 3.97 (m, 3H), 3.81 (dd, *J* = 13.3, 7.5, 1H), 3.64 (dd, *J* = 13.4, 4.0, 1H), 3.53 (m, 1H), 3.11 – 3.01 (m, 6H), 1.79 – 1.66 (m, 2H), 1.48 – 1.40 (m, 2H); ^{13}C NMR (150.9 MHz, CD_3OD) δ = 170.0, 169.6, 168.9, 159.5, 158.5, 137.3, 135.1, 133.9, 129.3, 128.7, 128.5, 128.44, 128.40, 127.2, 126.7, 57.3, 52.27, 52.26, 51.4, 49.5, 44.7, 41.6, 34.4, 29.8, 27.1, 26.3; HRMS (ESI): *m/z* $[M + 2H]^{2+}$ (z = 2) calcd for $C_{26}H_{37}N_9O_3S$:

227.6365; found: 227.6359; HRMS (ESI): *m/z* $[M + H]^+$ calcd for $C_{26}H_{36}N_9O_3S$: 554.2656; found: 554.2659.

4.1.10. (9*H*-fluoren-9-yl)methyl ((7*S*,10*S*)-3-methoxy-5-(2-(naphthalen-2-yl)ethyl)-6,9-dioxo-7-(3-(3-((2,2,4,6,7-pentamethyl-2,3-dihydrobenzofuran-5-yl)sulfonyl)guanidino)propyl)-13,13,13-triphenyl-2-oxa-12-thia-5,8-diazatridecan-10-yl)carbamate (26)

Et_2NH (7 mL) was added to a solution of the Fmoc-protected amine **23 (**308 mg, 0.33 mmol) in CH_2Cl_2 (7 mL) and the reaction was stirred for 3 h at room temperature with HPLC monitoring. The solvent was removed under reduced pressure and the crude product (320 mg) was used directly in the next step. HRMS (ESI): *m/z* $[M + H]^+$ calcd for $C_{35}H_{50}N_5O_6S$: 668.3476; found: 668.3488.

Fmoc-D-Cys(Trt)-OH (364 mg, 0.62 mmol), HATU (236 mg, 0.62 mmol) and DIPEA (0.25 mL, 1.4 mmol) were dissolved in CH_2Cl_2 (2 mL) and the resulting mixture was stirred for 30 min at room temperature, before a solution of crude Fmoc-deprotected **23** (320 mg, 0.48 mmol) in CH_2Cl_2 (3 mL) was added. The reaction mixture was stirred for 24 h at room temperature under anhydrous conditions ($CaCl_2$). After evaporation of the solvent the residue was partitioned between EtOAc (20 mL) and H_2O (40 mL). The aqueous layer was extracted with EtOAc (2 x 15 mL), and the combined organic layer was washed with 1M $KHSO_4$ (30 mL), H_2O (30 mL), saturated $NaHCO_3$ (30 mL), brine (30 mL) and was dried over anhydrous $MgSO_4$. Removal of the solvent under reduced pressure gave the crude product as a light red colored foam (710 mg). Purification by flash column chromatography (EtOAc/hexanes, 8:2) gave the title compound as a colorless foam (237 mg, 45% over two steps). R_f (EtOAc/hexane, 8:2) = 0.19; HRMS (ESI): *m/z* $[M + H]^+$ calcd for $C_{72}H_{78}N_6O_9S_2$: 1235.5344; found: 1235.5334.

4.1.11. *tert*-Butyl ((7*S*,10*S*)-3-methoxy-19,19-dimethyl-5-(2-(naphthalen-2-yl)ethyl)-6,9,12,17-tetraoxo-7-(3-(3-(2,2,4,6,7-pentamethyl-2,3-dihydrobenzofuran-5-ylsulfonyl)guanidino)-propyl)-10-(tritylthiomethyl)-2,18-dioxa-5,8,11,14,16-pentaazaicosan-15-ylidene)carbamate (27)

Et_2NH (6 mL) was added to a solution of the Fmoc-protected amine **26 (**237 mg, 0.19 mmol) in CH_2Cl_2 (6 mL) and the reaction was stirred for 3 h at room temperature with HPLC monitoring. The solvent was removed under reduced pressure and the crude product (277

mg), was used directly in the next step. HRMS (ESI): *m/z* $[M + H]^+$ calcd for $C_{57}H_{69}N_6O_7S_2$: 1013.4664; found: 1013.4663

To a solution of carboxylic acid **20** (150 mg, 0.47 mmol) in CH_2Cl_2 (2 mL), were added HATU (156 mg, 0.41 mmol) and DIPEA (0.15 mL, 0.82 mmol). The mixture was stirred at room temperature under anhydrous environment ($CaCl_2$) for 15 min before a solution of the Fmoc-deprotected amine **26** (277 mg, 0.27 mmol) in CH_2Cl_2 (2 mL) was added drop-wise to the reaction mixture, and stirring continued for 24 h. After evaporation of the solvent the residue was partitioned between EtOAc (20 mL) and H_2O (30 mL). The aqueous layer was extracted with EtOAc (2 x 15 mL), and the combined organic layer was washed with 1M $KHSO_4$ (30 mL), H_2O (30 mL), saturated $NaHCO_3$ (30 mL), brine (30 mL), and was dried over anhydrous $MgSO_4$. Removal of the solvent under reduced pressure gave the crude product (352 mg). Purification by flash column chromatography (EtOAc/hexanes, 9:1) gave the title compound (93 mg, 37% over 2 steps). R_f (EtOAc/hexane, 9:1) = 0.45; NMR analyses did not give useful information due to formation of rotamers; HRMS (ESI): *m/z* $[M + H]^+$ calcd for $C_{70}H_{89}N_9O_{12}S_2$: 1312.6145; found: 1312.6141.

4.1.12. 2-guanidino-*N*-((3*S*,6*S*,9a*S*)-6-(3-guanidinopropyl)-8-(2-(naphthalen-2-yl)ethyl)-4,7-dioxohexahydro-2*H*,6*H*-pyrazino[2,1-*b*][1,3]thiazin-3-yl)acetamide (12)

Linear precursor **27** (76 mg, 0.06 mmol) was dissolved in a mixture of TFA, thioanisole and distilled H_2O (90:5:5, 7 mL) and stirred for 2 h. After evaporation of the solvent under reduced pressure the brown residue was cooled to 0 °C. Addition of cold ether resulted in precipitation and the crude product was purified by preparative RP-HPLC, and lyophilized to give the title compound as a fluffy white solid (1.5 mg, 3%). ^{1}H NMR (600 MHz, CD_3OD): δ = 7.84 – 7.78 (m, 3H), 7.70 (s, 1H), 7.46 – 7.39 (m, 3H), 5.00 (dd, *J* = 11.0, 5.4, 1H), 4.72 (dd, *J* = 11.9, 6.3, 1H), 4.64 (t, *J* = 8.0, 1H), 4.15 – 4.08 (m, 1H), 3.99 (q, *J* = 29.4, 17.3, 2H), 3.70 – 3.55 (m, 3H), 3.36 (dd, *J* = 10.6, 6.3, 1H), 3.12 – 3.04 (m, 2H), 3.01 – 2.96 (m, 1H), 2.90 – 2.85 (m, 1H), 2.73 (t, *J* = 11.3, 1H), 1.67 – 1.58 (m, 1H), 1.56 – 1.49 (m, 1H), 1.31 – 1.24 (m, 2H); ^{13}C NMR (150.9 MHz, CD_3OD) δ = 170.5, 169.9, 169.3, 159.4, 158.4, 137.2, 135.0, 133.9, 129.3, 128.7, 128.6, 128.5, 128.4, 127.4, 126.8, 57.6, 52.8, 51.4, 48.9, 48.7, 44.6, 41.4, 34.7, 30.7, 28.5, 26.3; HRMS (ESI): *m/z* $[M + H]^+$ calcd for $C_{26}H_{35}N_9O_3S$; 554.2656; found: 554.2659.

4.1.13. 3-(Hydroxymethyl)piperidin-2-on (29)[28]

To a stirred suspension of ethyl 2-oxopiperidine-3-carboxylate (**28**) (1.00 g, 5.8 mmol) and anhydrous $CaCl_2$ (702 mg, 6.3 mmol) in dry MeOH (12 mL) in an ice/H_2O bath, $NaBH_4$ (501 mg, 13 mmol) was added in one portion, and stirring was continued for 2 h at 0 °C. After 16 h of additional stirring at room temperature, the solvent was evaporated, and a 3N aqueous citric acid solution was added in small portions until all solid material was dissolved (pH = 2-3). The solution was extracted with CH_2Cl_2 (6 x 50 mL), dried over Na_2SO_4 and filtered. Evaporation of the solvent gave the crude product (643 mg), which was purified by flash column chromatography on silica gel (5 % MeOH in EtOAc) to give the title compound as white solid (573 mg, 76 %). R_f (EtOAc) = 0.11; ^{1}H NMR (400 MHz, $CDCl_3$): δ = 5.99 (bs, 1H), 4.07 (d, *J* = 8.5, 1H), 3.81 – 3.60 (m, 2H), 3.39 – 3.21 (m, 2H), 2.56 – 2.42 (m, 1H), 1.97 – 1.71 (m, 3H), 1.56 – 1.39 (m, 1H); ^{13}C NMR (100 MHz, $CDCl_3$, 25°C): δ = 176.2, 64.9, 43.2, 42.0, 24.1, 22.3; HRMS (ESI): *m/z* $[M + H]^+$ calcd for $C_6H_{12}NO_2$: 130.0868; found: 130.0850.

4.1.14. 3-Methylenepiperidin-2-one (30)[28]

N,*N*'-Dicyclohexylcarbodiimide (DCC) (346 mg, 1.7 mmol) was added to a stirring solution of alcohol **29** (167 mg, 1.3 mmol) in dry toluene (2 mL). The mixture was heated at 110 °C (oil bath) and CuI (23 mg, 0.12 mmol) was added and the mixture was stirred for 70 min before it was cooled to room temperature, after which H_2O (1.6 mL) was added and stirring continued for 1 h. Et_2O (3.4 mL) was added, and the mixture was filtered. The aqueous phase was separated and extracted four times with 30 mL portions of CH_2Cl_2. The combined extracts were dried over K_2CO_3, filtered and evaporated to give the title compound as a white solid (144 mg, 100 %). R_f (EtOAc) = 0.17; ^{1}H NMR (400 MHz, $CDCl_3$): δ = 6.91 (bs, 1H), 6.21 (bs, 1H), 5.37 – 5.26 (m, 1H), 3.40 (td, *J* = 6.2, 2.6, 2H), 2.67 – 2.51 (m, 2H), 1.95 – 1.79 (m, 2H); ^{13}C NMR (100 MHz, $CDCl_3$): δ = 166.6, 138.1, 122.5, 43.2, 30.4, 23.7; HRMS (ESI): *m/z* $[M + H]^+$ calcd for $C_6H_{10}NO$: 112.0762; found: 112.0779.

4.1.15. *tert*-Butyl 3-methylene-2-oxopiperidine-1-carboxylate (31)

Et_3N (1.2 mL, 8.8 mmol) and DMAP (1.07 g, 8.8 mmol) were added to a stirring solution of lactam **30** (971 mg, 8.7 mmol) in dry CH_2Cl_2/DMF (10:1, 27 mL). Boc_2O (3.83 g, 17 mmol) in CH_2Cl_2 (12 mL) was added drop-wise, and the reaction mixture was stirred at room temperature for 14 h. The mixture was concentrated and purified by flash column chromatography on silica gel (EtOAc/hexane 1:4) to give the title compound (1.72 g, 94 %)

as transparent thick oil. R_f (EtOAc/hexane 1:4) = 0.34; ^{1}H NMR (400 MHz, $CDCl_3$): δ = 6.33 (d, *J* = 1.4, 1H), 5.41 (d, *J* = 0.7, 1H), 3.78 – 3.67 (m, 2H), 2.58 (t, *J* = 6.1, 2H), 1.95 – 1.84 (m, 2H), 1.55 (s, 9H); ^{13}C NMR (100 MHz, $CDCl_3$): δ = 164.8, 153.3, 138.8, 125.1, 83.1, 46.9, 29.5, 28.2, 22.8; HRMS (ESI): *m/z* $[M + Na]^+$ calcd for $C_{11}H_{17}NO_3Na$: 234.1102; found: 234.1101.

4.1.16. *tert*-Butyl 2-oxo-3-(tritylthiomethyl)piperidine-1-carboxylate (32)

To a stirred solution of lactam **31** (1.65 g, 7.8 mmol) in dry CH_2Cl_2 (33 mL) was added Ph_3CSH (2.16 g, 7.8 mmol) and Et_3N (1.1 mL, 7.8 mmol) and the resulting mixture was stirred at room temperature for 12 h. The reaction mixture was washed with H_2O, concentrated and purified by flash column chromatography on silica gel (hexane/EtOAc 8:2) to give the title compound as white foam (3.60 g, 95 %). R_f (hexane/EtOAc 4:1) = 0.18; ^{1}H NMR (400 MHz, $CDCl_3$): δ = δ 7.45 – 7.20 (m, 15H), 3.76 – 3.66 (m, 1H), 3.34 (ddd, *J* = 12.9, 7.6, 5.1, 1H), 2.88 (dd, *J* = 12.7, 4.6, 1H), 2.28 (dd, *J* = 12.7, 8.6, 1H), 2.09 – 1.97 (m, 1H), 1.95 – 1.81 (m, 1H), 1.75 – 1.65 (m, 2H), 1.49 (s, 9H), 1.33 – 1.26 (m, 1H); ^{13}C NMR (100 MHz, $CDCl_3$): δ = 172.8, 152.9, 145.0, 129.9, 128.1, 126.9, 83.2, 67.1, 45.1, 43.6, 33.0, 28.2, 25.5, 21.7; HRMS (ESI): *m/z* $[M + Na]^+$ calcd for $C_{30}H_{33}NO_3SNa$: 510.2073; found: 510.2070.

4.1.17. 5-(*tert*-Butoxycarbonylamino)-2-((tritylthio)methyl)pentanoic acid (33)

To a stirred solution of lactam **32** (3.60 g, 7.4 mmol) in THF (37 mL), was added LiOH (1.0 M, 15 mL, 15 mmol). The reaction was monitored by TLC and all starting material was consumed after 1h. The THF was evaporated and the aqueous residue was acidified to pH 4 with 10% citric acid. The mixture was extracted with CH_2Cl_2 (4 x 50 mL), dried over $MgSO_4$, filtered and evaporated to give the title compound as white foam (3.52 g, 94%). R_f (hexane/EtOAc 6:4) = 0.20; ^{1}H NMR (400 MHz, $CDCl_3$): δ = 7.46 – 7.17 (m, 15H), 4.47 (bs, 1H), 2.97 (bs, 2H), 2.61 (dd, *J* = 12.5, 8.1 Hz, 1H), 2.22 (dd, *J* = 12.6, 6.1 Hz, 1H), 2.11 – 1.99 (m, 1H), 1.50 – 1.33 (s and m, 11H), 1.26 (m, 2H); ^{13}C NMR (100 MHz, $CDCl_3$): δ = 179.8, 156.2, 144.8, 129.9, 128.2, 127.0, 79.5, 67.2, 44.9, 40.3, 33.3, 29.0, 28.6, 27.5; HRMS (ESI): *m/z* $[M + Na]^+$ calcd for $C_{30}H_{35}NO_4SNa$: 528.2184; found: 528.2174.

4.1.18. *tert*-Butyl ((*SR*)-5-(((*S*)-1-((2,2-dimethoxyethyl)(2-(naphthalen-2-yl)ethyl)amino)-1-oxo-5-(3-((2,2,4,6,7-pentamethyl-2,3-dihydrobenzofuran-5-yl)sulfonyl)guanidino)pentan-2-yl)amino)-5-oxo-4-((tritylthio)methyl)pentyl)carbamate (34)

Et_2HN (1.9 mL, 18 mmol) was added to a stirring solution of **23** (334 mg, 3.8 mmol) in CH_2Cl_2 (3.9 mL) at room temperature. The reaction was monitored by TLC and deemed completed after 3 h. The mixture was evaporated to dryness and the residue used in the following step.

To a stirred solution of carboxylic acid **33** (182 mg, 0.36 mmol) in dry CH_2Cl_2 (2.1 mL), were added HBTU (142 mg, 0.38 mmol) and DIPEA (66 µL, 0.38 mmol) and the mixture was stirred for 30 min. Fmoc-deprotected amine **23** (250 mg out of 344 mg crude product, 0.38 mmol) in dry CH_2Cl_2 (2.1 mL) was added and stirring continued for 17 h. The solvent was evaporated to give red foam, which was partitioned between EtOAc (20 mL) and H_2O (10 mL). The organic phase was separated and washed with 5% $KHSO_4$ (10 mL) and brine (10 mL). The organic phase was further concentrated and purified by flash chromatography on silica gel (EtOAc/hexane 3:1) to give an inseparable mixture of the two diastereoisomers of **34** as white foam (352 mg, 85 %). The product retained EtOAc and the yield is adjusted accordingly. R_f (EtOAc/hexane, 3:1) = 0.29; HRMS (ESI): *m/z* $[M + H]^+$ calcd for $C_{65}H_{83}N_6O_9S_2$: 1155.5658; found: 1155.5667; HRMS (ESI): *m/z* $[M + Na]^+$ calcd for $C_{65}H_{82}N_6O_9S_2Na$: 1177.5477; found: 1177.5474.

4.1.19. 1,1'-(((3*R*,6*S*,9a*S*)-8-(2-(Naphthalen-2-yl)ethyl)-4,7-dioxohexahydro-2*H*,6*H*-pyrazino[2,1-*b*][1,3]thiazine-3,6-diyl)bis(propane-3,1-diyl))diguanidine (13)

The diastereoisomeric mixture of linear precursor **34** (925 mg, 0.8 mmol) was dissolved in a mixture of TFA, thioanisole and H_2O (90:5:5, 28 mL) and the resulting mixture was stirred at room temperature for 90 min. The TFA mixture was evaporated and the crude product was precipitated by addition of cold diethyl ether. The ether was drained off and the residue was dried in vacuo to give the crude product as a reddish solid (422 mg). The crude product (210 mg, approx. 0.43 mmol) in dry DMF (3.5 mL) was added 1*H*-pyrazole-1-carboxamidine hydrochloride (92 mg, 0.63 mmol) and DIPEA (0.11 mL, 0.63 mmol), and the mixture was stirred under argon atmosphere for 72 h during which the reaction was monitored by RP-HPLC. Diethyl ether (30 mL) was then added and the mixture was cooled at 4 °C and stirred for an additional hour, resulting in the precipitation of a white solid (230 mg). The crude product was purified by preparative HPLC to give the title compound as a fluffy white solid

(11 mg, 7%). ^{1}H NMR (600 MHz, CD_3OD) δ = 7.82 – 7.77 (m, 3H), 7.69 (s, 1H), 7.47 – 7.40 (m, 3H), 5.14 (dd, *J* = 5.4, 4.6, 1H), 4.00 (dt, *J* = 13.6, 7.7, 1H), 3.70 (dd, *J* = 13.9, 4.0, 1H), 3.58 – 3.51 (m, 2H), 3.17 (t, *J* = 7.0, 2H), 3.10 – 3.98 (m, 5H), 2.78 – 2.73 (m, 1H), 2.58 (t, *J* = 12.0, 1H), 1.91 – 1.85 (m, 1H), 1.68 – 1.56 (m, 4H), 1.46 – 1.41 (m, 1H), 1.40 – 1.35 (m, 3H); ^{13}C NMR (150.9 MHz, CD_3OD) δ = 173.8, 169.4, 158.7, 158.5, 137.3, 135.0, 133.8, 129.3, 128.7, 128.51, 128.49, 128.45, 127.2, 126.7, 56.6, 52.9, 50.9 (HSQC), 49.3 (HSQC), 43.8, 42.4, 41.6, 34.4, 30.2, 28.9, 28.6, 27.5, 26.2; HRMS (ESI): *m/z* $[M + H]^+$ calcd for $C_{27}H_{39}N_8O_2S$: 539.2911; found: 539.2906.

4.1.20. 1,1'-(((3*S*,6*S*,9a*R*)-8-(2-(Naphthalen-2-yl)ethyl)-4,7-dioxohexahydro-2*H*,6*H*-pyrazino[2,1-*b*][1,3]thiazine-3,6-diyl)bis(propane-3,1-diyl))diguanidine (14)

Bicycle **14** was prepared as described for **13**. The crude was purified by preparative HPLC to give the title compound as a fluffy white solid (16 mg, 11%). ^{1}H NMR (600 MHz, CD_3OD) δ = 7.84 – 7.80 (m, 2H), 7.78 (d, *J* = 7.7, 1H), 7.67 (d, 1H), 7.47 – 7.43 (m, 3H), 4.68 – 4.62 (m, 2H), 4.08 – 4.02 (m, 1H), 3.68 (dt, *J* = 13.6, 5.9, 1H), 3.60 (d, *J* = 9.1, 2H), 3.19 – 3.14 (m, 3H), 3.08 (t, *J* = 6.7, 2H), 3.00 – 2.95 (m, 1H), 2.94 – 2.90 (m, 1H), 2.55 (t, *J* = 11.4, 1H), 2.41 – 2.36 (m, 1H), 1.85 – 1.79 (m, 1H), 1.65 – 1.57 (m, 3H), 1.53 – 1.46 (m, 1H), 1.45 – 1.39 (m, 1H), 1.33 – 1.25 (m, 2H); ^{13}C NMR (150.9 MHz, CD_3OD) δ = 174.1, 170.4, 158.7, 158.5, 137.3, 134.9, 133.8, 129.3, 128.73, 128.70, 128.42, 128.41, 127.4, 126.8, 57.1, 53.7, 49.0 (HSQC), 48.9 (HSQC), 42.8, 42.4, 41.5, 34.6, 30.7, 29.9, 28.8, 27.7, 26.3; HRMS (ESI): *m/z* $[M + H]^+$ calcd for $C_{27}H_{39}N_8O_2S$: 539.2911; found: 539.2905.

4.2. Molecular modeling.

The conformational search for scaffolds **A** and **A'** was performed using the MacroModel application as integrated in Schrödinger Suite 2012,[29] running on a Dell Precision 390 workstation. The OPLS_2005 force field and the GB/SA solvent model for water were used for the energy calculations. The Truncated Newton Conjugate Gradient (TNCG) algorithm was used for the energy minimizations, with maximum 500 iterations and a convergence threshold of 0.012 kcal/mol×Å (0.05 kJ/mol×Å). The Monte Carlo Multiple Minimum (MCMM) search algorithm was used for torsional sampling (1000 steps), and the energy cutoff was set to 5 kcal/mol (21 kJ/mol) above the lowest energy conformation. Mirror image conformations were retained, and redundant conformations were eliminated by using an RMSD cutoff (all atoms) of 0.5 Å. For both scaffolds, this resulted in four low-energy conformations, which were superimposed on the backbone of our previously reported 3D

pharmacophore model for cyclopentapeptide CXCR4 antagonists using five atoms: the α-carbon atoms of Arg^1, Arg^2, and 2-Nal^3 and the β-carbon atoms of Arg^1 and Arg^2.

4.3. Biological Studies.

4.3.1. Transfections and tissue culture.

COS-7 cells were grown in Dulbecco's modified Eagle's medium (DMEM) with Glutamax (Invitrogen, UK) supplemented with 10% fetal bovine serum (FBS), 180 units/mL penicillin and 45 μg/mL streptomycin (PenStrep) at 37 °C in a 10% CO_2/90% humidified atmosphere. Transfection of cells was carried out by the calcium phosphate precipitation method.[30,31] Briefly, plasmid DNA (20 μg of receptor cDNA and 30 μg of the chimeric $G\alpha_i$ to $G\alpha_q$ signal-converting G protein $G\alpha_{\Delta 6qi4myr}$) were mixed with TE-buffer (10 mM Tris-HCl, 2 mM Na_2EDTA, pH 7.5) and 30 μL calcium chloride (2 M) to a total volume of 480 μL, and then added to the same amount of HEPES buffered saline (280 mM NaCl, 50 mM HEPES, 1.5 mM Na_2HPO_4, pH 7.2). Precipitation was allowed for 45 min at room temperature, after which the precipitate together with 300 μL chloroquine (2 mg/mL) in 10 mL culture media was added to the 6×10^6 COS-7 cells seeded the day before. Transfection was stopped after 5 h by replacing media, and cells were incubated overnight.

4.3.2. Functional assay.

The potency was measured using a scintillation proximity-based inositol-phosphate accumulation assay (SPA-IP).[32] In brief, one day after transfection COS-7 cells (0.35×10^5 cells/well) were incubated for 24 h with [^{3}H]-myo-inositol (5 μL/mL, 2 μCi/mL) in 0.1 mL of growth medium per well in a 96-well plate. The following day, cells were washed twice in PBS and were incubated in 0.1 mL of Hank's balanced salt solution (Invitrogen, U.K.) supplemented with 10 mM LiCl at 37 °C in the presence of various concentrations of ligands for 90 min. Cells were extracted by addition of 50 μL of 10 mM formic acid to each well, followed by incubation on ice for 30−60 min. The [^{3}H]inositol-phosphates in the formic acid cell lysates were quantified by Ysi-poly-D-Lys coated SPA beads. Briefly, 35 μL of cell extract was mixed with 80 μL of a SPA bead suspension (12.5 μg/μL in H_2O) in a PicoPlate-96 white plate. Plates were sealed, agitated for at least 30 min and centrifuged (5 min, 1500 rpm). SPA beads were allowed to settle and react with the extract for 8 h before radioactivity was determined using a Packard Top Count NXT™ scintillation counter (PerkinElmer, MA, USA). All determinations were made in duplicate. This readout has earlier been used effectively for CXCR4 and other chemokine receptors.[13,33]

SUPPLEMENTARY DATA

Experimental procedures for **4**–**10** and relevant sections of ROESY spectra for compounds **11**–**14** can be found in the online version, at http://

ACKNOWLEDGMENT

Financial support for this project was obtained from UiT The Arctic University of Norway (Z.G.Z. and J.V.), the University of Bergen and L. Meltzers Høyskolefond (B.E.H.), and from the University of Copenhagen and the Danish Medical Research Council (S.T. and M.M.R). We would also like to thank Inger S. Simonsen and Randi Thøgersen for invaluable technical assistance in the biological assay.

ABBREVIATIONS

2-Nal, L-3-(2-naphthyl)alanine; CXCL12, CXC chemokine ligand 12; CXCR4, CXC chemokine receptor 4; DIPEA, *N*,*N*-diisopropylethylamine; EDC, *N*-(3-dimethylaminopropyl)-*N*′-ethylcarbodiimide; HATU, 1-[bis(dimethylamino)methylene]-1*H*-1,2,3-triazolo[4,5-*b*]pyridinium-3-oxide hexafluorophosphate; HBTU, 1-[bis(dimethylamino) methylene]-1*H*-benzotriazolium-3-oxide hexafluorophosphate; HFIP, 1,1,1,3,3,3-hexafluoroisopropanol; HOBt, 1-hydroxybenzotriazole; Pbf, 2,2,4,6,7-pentamethyl-2,3-dihydrobenzofuran-5-sulfonyl; PyBOP, (benzotriazol-1-yloxy)tripyrrolidinophosphonium hexafluorophosphate; SPPS, solid phase peptide synthesis; TIS, triisopropylsilane; Trt, triphenylmethyl.

REFERENCES AND NOTES

1. Bleul, C. C.; Farzan, M.; Choe, H.; Parolin, C.; Clark-Lewis, I.; Sodroski, J.; Springer, T. A. *Nature* **1996**, *382*, 829.
2. Oberlin, E.; Amara, A.; Bachelerie, F.; Bessia, C.; Virelizier, J. L.; Arenzana-Seisdedos, F.; Schwartz, O.; Heard, J. M.; Clark-Lewis, I.; Legler, D. F.; Loetscher, M.; Baggiolini, M.; Moser, B. *Nature* **1996**, *382*, 833.
3. Debnath, B.; Xu, S.; Grande, F.; Garofalo, A.; Neamati, N. *Theranostics* **2013**, *3*, 47.
4. Mosley, C. A.; Wilson, L. J.; Wiseman, J. M.; Skudlarek, J. W.; Liotta, D. C. *Expert Opin. Ther. Pat.* **2009**, *19*, 23.

5. Fujii, N.; Oishi, S.; Hiramatsu, K.; Araki, T.; Ueda, S.; Tamamura, H.; Otaka, A.; Kusano, S.; Terakubo, S.; Nakashima, H.; Broach, J. A.; Trent, J. O.; Wang, Z. X.; Peiper, S. C. *Angew. Chem. Int. Ed.* **2003**, *42*, 3251.
6. Stradley, S. J.; Rizo, J.; Bruch, M. D.; Stroup, A. N.; Gierasch, L. M. *Biopolymers* **1990**, *29*, 263.
7. Ruiz-Gomez, G.; Tyndall, J. D.; Pfeiffer, B.; Abbenante, G.; Fairlie, D. P. *Chem. Rev.* **2010**, *110*, PR1.
8. Ripka, A. S.; Rich, D. H. *Curr. Opin. Chem. Biol.* **1998**, *2*, 441.
9. Ung, P.; Winkler, D. A. *J. Med. Chem.* **2011**, *54*, 1111.
10. Ueda, S.; Oishi, S.; Wang, Z. X.; Araki, T.; Tamamura, H.; Cluzeau, J.; Ohno, H.; Kusano, S.; Nakashima, H.; Trent, J. O.; Peiper, S. C.; Fujii, N. *J. Med. Chem.* **2007**, *50*, 192.
11. Mungalpara, J.; Zachariassen, Z. G.; Thiele, S.; Rosenkilde, M. M.; Våbenø, J. *Org. Biomol. Chem.* **2013**, *11*, 8202.
12. Tamamura, H.; Esaka, A.; Ogawa, T.; Araki, T.; Ueda, S.; Wang, Z.; Trent, J. O.; Tsutsumi, H.; Masuno, H.; Nakashima, H.; Yamamoto, N.; Peiper, S. C.; Otaka, A.; Fujii, N. *Org. Biomol. Chem.* **2005**, *3*, 4392.
13. Mungalpara, J.; Thiele, S.; Eriksen, Ø.; Eksteen, J.; Rosenkilde, M. M.; Våbenø, J. *J. Med. Chem.* **2012**, *55*, 10287.
14. Tamamura, H.; Araki, T.; Ueda, S.; Wang, Z.; Oishi, S.; Esaka, A.; Trent, J. O.; Nakashima, H.; Yamamoto, N.; Peiper, S. C.; Otaka, A.; Fujii, N. *J. Med. Chem.* **2005**, *48*, 3280.
15. White, C. J.; Yudin, A. K. *Nat. Chem.* **2011**, *3*, 509.
16. Tamamura, H.; Tsutsumi, H.; Masuno, H.; Mizokami, S.; Hiramatsu, K.; Wang, Z.; Trent, J. O.; Nakashima, H.; Yamamoto, N.; Peiper, S. C.; Fujii, N. *Org. Biomol. Chem.* **2006**, *4*, 2354.
17. Narumi, T.; Tanaka, T.; Hashimoto, C.; Nomura, W.; Aikawa, H.; Sohma, A.; Itotani, K.; Kawamata, M.; Murakami, T.; Yamamoto, N.; Tamamura, H. *Bioorg. Med. Chem. Lett.* **2012**, *22*, 4169.
18. Våbenø, J.; Nikiforovich, G. V.; Marshall, G. R. *Biopolymers* **2006**, *84*, 459.
19. Che, Y.; Marshall, G. R. *Expert Opin. Ther. Targets* **2008**, *12*, 101.
20. In previous publications these structures have been denoted as being 3,8,10-trisubstituted.
21. Vojkovsky, T.; Weichsel, A.; Patek, M. *J. Org. Chem.* **1998**, *63*, 3162.

22. Kohn, W. D.; Zhang, L. *Tetrahedron Lett.* **2001**, *42*, 4453.
23. Grimes, J., John H.; Zheng, W.; Kohn, W. D. *Tetrahedron Lett.* **2004**, *45*, 6333.
24. Niida, A.; Tanigaki, H.; Inokuchi, E.; Sasaki, Y.; Oishi, S.; Ohno, H.; Tamamura, H.; Wang, Z.; Peiper, S. C.; Kitaura, K.; Otaka, A.; Fujii, N. *J. Org. Chem.* **2006**, *71*, 3942.
25. Ueda, S.; Kato, M.; Inuki, S.; Ohno, H.; Evans, B.; Wang, Z.-x.; Peiper, S. C.; Izumi, K.; Kodama, E.; Matsuoka, M.; Nagasawa, H.; Oishi, S.; Fujii, N. *Bioorg. Med. Chem. Lett.* **2008**, *18*, 4124.
26. Allen, M. J.; Raines, R. T.; Kiessling, L. L. *J. Am. Chem. Soc.* **2006**, *128*, 6534.
27. Balakrishnan, S.; Zhao, C.; Zondlo, N. J. *J. Org. Chem.* **2007**, *72*, 9834.
28. Klutchko, S.; Hoefle, M. L.; Smith, R. D.; Essenburg, A. D.; Parker, R. B.; Nemeth, V. L.; Ryan, M. J.; Dugan, D. H.; Kaplan, H. R. *J. Med. Chem.* **1981**, *24*, 104.
29. MacroModel, version 9.9, Schrödinger, LLC, New York, NY, 2012.
30. Kissow, H.; Hartmann, B.; Holst, J. J.; Viby, N. E.; Hansen, L. S.; Rosenkilde, M. M.; Hare, K. J.; Poulsen, S. S. *Regul. Pept.* **2012**, *179*, 91.
31. Rosenkilde, M. M.; Cahir, M.; Gether, U.; Hjorth, S. A.; Schwartz, T. W. *J. Biol. Chem.* **1994**, *269*, 28160.
32. Brandish, P. E.; Hill, L. A.; Zheng, W.; Scolnick, E. M. *Anal. Biochem.* **2003**, *313*, 311.
33. Thiele, S.; Malmgaard-Clausen, M.; Engel-Andreasen, J.; Steen, A.; Rummel, P. C.; Nielsen, M. C.; Gloriam, D. E.; Frimurer, T. M.; Ulven, T.; Rosenkilde, M. M. *J. Med. Chem.* **2012**, *55*, 8164.

BMC-D-14-00355 revised

Graphical Abstract